Low-frequency response of pinned charge-density-wave condensates

Wei-Yu Wu, L. Mihaly, George Mozurkewich,* and G. Gruner
Department of Physics and Solid State Science Center, University of California, Los Angeles, Los Angeles, California 90024
(Received 16 September 1985)

The frequency-dependent conductivity $\sigma(\omega)$ was investigated in the 10 Hz to ~500 MHz range in materials with an incommensurate charge-density wave. $NbSe_3$, orthorhombic TaS_3, and $(TaSe_4)_2I$. Over a wide range of frequencies both $\mathrm{Re}\sigma(\omega)$ and $\mathrm{Im}\sigma(\omega)$ are described by the expression $\sigma(\omega)=C(i\omega/\bar{\omega})^{\alpha}$ with $\alpha<1$, and have different values for each material. The ω-dependent response is in clear disagreement with descriptions which neglect the internal degrees of freedom of the condensate. The excess low-frequency conductivity is due to the disorder caused by random distribution of pinning centers. The results are compared with calculations based on a microscopic phase Hamiltonian, which takes impurity pinning into account. The results are in semiquantitative agreement with a modified form of the Mott-Berezhinskii law for one-dimensional hopping conductivity, and they are in qualitative agreement with the classical, relaxational dynamics approach in the $\omega\rightarrow 0$ limit. We also discuss the relation of our experimental findings to other studies of the frequency-dependent response in these materials.

I. INTRODUCTION

The highly anomalous transport properties which arise as a consequence of the development of incommensurate charge-density waves (CDW's) in metallic quasi-one-dimensional compounds are of considerable current interest.[1,2] It is by now well established that in certain inorganic linear chain compounds, such as $NbSe_3$ or orthorombic TaS_3 (o-TaS_3), the collective mode is pinned by impurities, grain boundaries, etc. This results in zero dc CDW conduction for small applied electric fields. The interaction between the CDW and the pinning centers is weak, however, and the characteristic pinning energy can be orders of magnitude smaller than the relevant single-particle energies such as the band gap or bandwidth. Consequently, the pinned mode displays strongly-frequency-dependent response and associated giant dielectric constant in the spectral region between audio and millimeter wave frequencies.[3–21] In general, the in-phase part of the conductivity $\mathrm{Re}\sigma(\omega)$ smoothly increases with increasing frequency in the megahertz frequency region, and has a broad maximum at millimeter wave frequencies. The out-of-phase component, $\mathrm{Im}\sigma(\omega)$, has a maximum where $\mathrm{Re}\sigma(\omega)$ strongly increases with increasing ω, and it crosses zero where $\mathrm{Re}\sigma(\omega)$ has it's maximum, being negative at high frequencies.

Several models have been advanced to account for this typical behavior. In one model,[22] the equation of motion for the average CDW phase is that of a classical damped harmonic oscillator. Another approach[23] interprets the strongly-frequency-dependent conductivity in terms of coherent Zener tunneling of CDW electrons through a small pinning gap, Δ_p. This so-called "tunneling model" leads to a scaling relation between the frequency- and voltage-dependent conductivities, which is well obeyed in the radio-frequency range both in $NbSe_3$ and in TaS_3.[24,25] Figure 1 illustrates the overall good agreement between their predictions and experimental data in $NbSe_3$. (For the situation in the microwave and millimeter spectral range, see Ref. 26). The details of the figure will be discussed in Sec. IV. Here we emphasize that both of these approaches neglect the local deformations of the collective mode around the various pinning centers, and the resulting loss of long-range phase coherence. Consequently, pinning is described by a single parameter: an average pinning frequency ω_0 or an average pinning gap Δ_p. Yet various studies on irradiated materials[27] and on alloys[28] indicate that randomly distributed impurities play a fundamental role in the observed frequency and electric

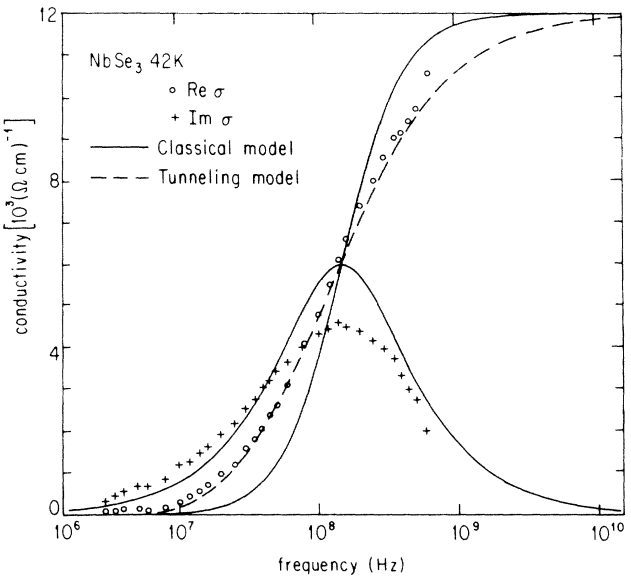

FIG. 1. $\mathrm{Re}\sigma(\omega)$ and $\mathrm{Im}\sigma(\omega)$ for $NbSe_3$ at 42 K. The solid lines are fits to classical harmonic-oscillator description, Eqs. (4) and (5) with parameters $\sigma_\infty=1.2\times10^4$ $(\Omega\,\mathrm{cm})^{-1}$, $\omega_{co}/2\pi=150$ MHz. The dashed line is a fit to tunneling model Eq. (6) with $\omega_T/2\pi=50$ MHz and E_0/E as given by Ref. 44.

 ©1986 The American Physical Society

field-dependent response. This in turn suggests that the dynamics of internal deformations may play an important role.

It is the principal goal of this paper to document the effects of the random distribution of pinning centers on the low-frequency conductivity by incommensurate CDW's. We report extensive complex conductivity measurements over a broad frequency range (100 Hz) to 500 MHz) in three model compounds for CDW conduction: $NbSe_3$, orthorhomic TaS_3 (o-TaS_3), and $(TaSe_4)_2I$. In all cases, at low frequencies the conductivity can be approximately described by the empirical form:

$$\sigma(\omega)=C\left[\frac{i\omega}{\bar{\omega}}\right]^{\alpha}, \quad \alpha<1 \tag{1}$$

over a broad range of frequencies below the peak in $\mathrm{Im}\sigma$. The exponent $\alpha<1$ varies from material to material and is only weakly temperature dependent. At frequencies between 10^2 and 10^5 Hz both $\mathrm{Re}\sigma(\omega)$ and $\mathrm{Im}\sigma(\omega)$ exceed the predictions of both the classical and tunneling models by orders of magnitude. Equation (1) is often observed in glassy materials,[29] and its applicability to CDW conductors demonstrates, in general, the importance of randomness in these materials.

The power-law form is entirely empirical; it is likely that the true form for $\sigma(\omega)$ has some other functional dependence which may be approximated by Eq. (1) over the relevant range of frequency. For example, it may be regarded as a limiting case of some Cole-Cole or Cole-Davidson–like function.[30] While the latter forms are equally empirical, they have been motivated on the basis of distributions of material parameters, such as relaxation times or characteristic energies.[29] From this perspective the connection between Eq. (1) and randomness begins to take shape. However, we prefer to look for a more microscopic origin to the low-frequency behavior. The disorder is expected to lead to metastable states[31] associated with regions of the CDW which are more weakly pinned than the average. One can visualize at least two ways in which these metastable states can contribute to the conductivity. (1) If two metastable states are spatially well separated but close in energy, then the low-frequency conductivity may be enhanced with a frequency-dependent response similar to that obtained for single-particle localized states (e.g., the Mott-Berezhinskii) law.[32–34] (2) If two metastable states are near neighbors, the potential-energy barriers between them (due to randomness) have a distribution of heights. In the thermodynamic limit, the distribution may extend nearly to zero,[31] and thermal activation over these barriers will introduce a cusplike enhancement into the low-frequency dielectric constant.[31,35] The same two processes are relevant to interpreting the long-time-scale relaxations which follow current pulses[36] or thermal quenches.[37]

The outline of the paper is as follows. After discussing the experimental methods and details in Sec. II, the experimental results observed in $NbSe_3$, o-TaS_3, and $(TaSe_4)_2I$ will be presented in Sec. III. This will be followed in Sec. IV by a detailed comparison of the experimental results with the various theories of frequency-dependent transport in pinned charge-density-wave systems. Our conclusions are summarized in Sec. V.

Short accounts of our experimental findings on the low-frequency behavior of the conductivity have been reported earlier.[16,21]

II. EXPERIMENTAL METHODS

$NbSe_3$, orthorhombic TaS_3 (o-TaS_3), and $(TaSe_4)_2I$ samples used in this study were prepared by the gradient furnace method. High-purity starting materials were sealed in an evacuated quartz tube and held at the growth temperature for a time extending from a few days to a few weeks. The temperature dependence of dc resistance and threshold field of nonlinear conductivity indicate that our specimens have a purity comparable to those reported in the literature. The typical sample dimensions are 20 μm$\times$5 μm$\times$1.5 mm, the long axis being the chain direction.

Electrical contacts were made by using silver paint or, in the case of $(TaSe_4)_2I$, by platinum paint or evaporated gold. Four-probe dc measurements indicated that the contact resistance was always much less than the sample resistance. We also found that for o-TaS_3, the contact resistance is temperature dependent. It may increase from a few ohms to a few hundred ohms as the sample is cooled from room temperature to 77 K, but it remains much smaller than the dc resistance of the sample. Several specimens with widely differing resistances were investigated to ensure that contact effects do not play a role in the experimental results. Furthermore, at low frequencies both four-probe and two-probe configurations were used with identical results.

In order to cover a large frequency range, several different methods were used to measure the complex conductivity. At high frequencies (4–500 MHz) a Hewlett-Packard HP8754 network analyzer was used. The impedance of the specimens was compared with a 50-Ω resistive impedance, and consequently highest accuracy was achieved for samples with impedance of the same order of magnitude. Careful calibration using both resistive and capacitive components was required, especially at the higher frequencies where the effect of finite cable lengths became important. At intermediate frequencies (500 kHz to 100 MHz) an rf bridge circuit built by us was employed. The voltage drop across the specimen was compared to a variable capacitor (varactor) and a variable resistor (trimmer potentiometer) in the other arm of the bridge. Again, calibration at each frequency was necessary. The calibration was performed immediately after each experimental run by substituting for the sample discrete resistive and capacitive components, whose values of R and C were appropriate to the observed range of sample admittances.

The total admittance of the specimens Y_T was assumed to consist of G_N, the (real) conductance of normal electrons thermally excited across the CDW gap, in parallel with Y_{CDW}, the (complex) CDW admittance, $Y_T = G_N + Y_{CDW}$. When either the network analyzer or the rf bridge was used, the separately measured dc, linear conductance G_N was subtracted numerically after the total

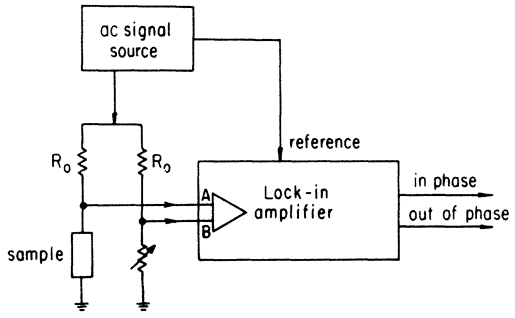

FIG. 2. Bridge configuration employed to measure the low-frequency conductivity.

admittance of the sample was determined. Because both CDW contributions Reσ and Imσ decrease rapidly with decreasing ω, Y_T and G_N become comparable in magnitude at low frequency, and the numerical subtraction becomes more susceptible to errors. Therefore, measurements below 100 kHz were performed with bridge circuits where the normal electron contribution is balanced out. One such circuit which we used was described in Ref. 6. Another very simple arrangement using the differential input of a Princeton Applied Research PAR 5204 lock-in amplifier is depicted in Fig. 2. At any given temperature either circuit was first balanced using dc applied fields. At finite frequencies the lock-in amplifier detects an unbalance voltage which is due to the CDW contribution to the conductivity. The in-phase and out-of-phase components of the measured voltage were used to calculate Re$\sigma(\omega)$ and Im$\sigma(\omega)$. We note that Reσ obtained in this way is subject to a error which decreases with increasing frequency. But no error is introduced into the out-of-phase component Imσ, and, most importantly, our sensitivity to small values of Reσ was increased by orders of magnitude by using this technique.

Accurate results can be obtained only after minimizing the stray capacitances in the measuring circuit. In order to reduce the spurious capacitive effects various gas flow systems were designed with typical cable lengths of 10 cm or less. Temperature stability is also important, especially at low frequencies where the conduction is dominated by the strongly-temperature-dependent dc conductance, G_N. To solve this problem, we built a liquid-N_2-cooled mini-cryostat, with temperature stability of 3×10^{-2} K in the temperature range of 80–200 K.

CDW conductors are inherently nonlinear systems, and nonlinear ac response has recently been reported in a related system $K_{0.3}MoO_3$, and also for o-TaS_3.[38] In Fig. 3 we show our data for the dependence of Imσ on amplitude V_{ac} of the ac driving voltage. While the CDW response is presumably nonlinear down to the lowest values of V_{ac}, this data indicates that Imσ is independent of V_{ac} within our experimental error for values approximately $V_{ac}<0.4V_T$. Further studies of the nonlinear response will be published separately. All experimental results reported in the rest of this paper were measured with $V_{ac}\leq0.1V_T$ and therefore are expected to represent the linear ac response to good accuracy.

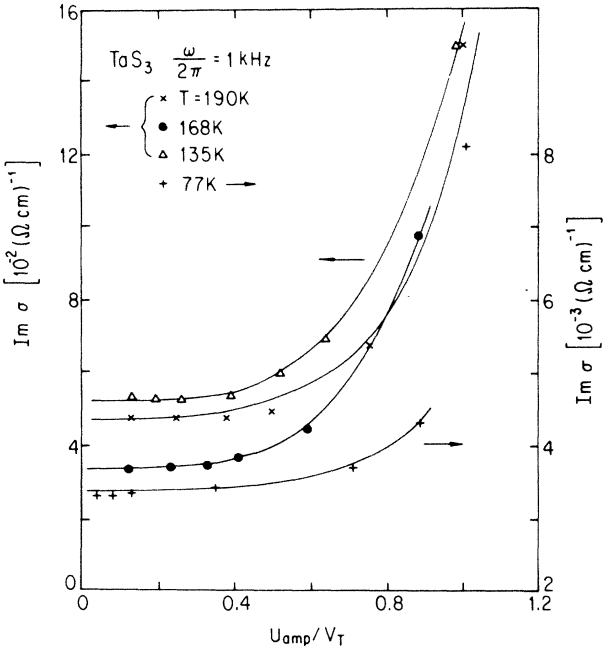

FIG. 3. The ac amplitude dependence of the CDW conductivity detected in o-TaS_3 at $f=1$ kHz and at several temperatures.

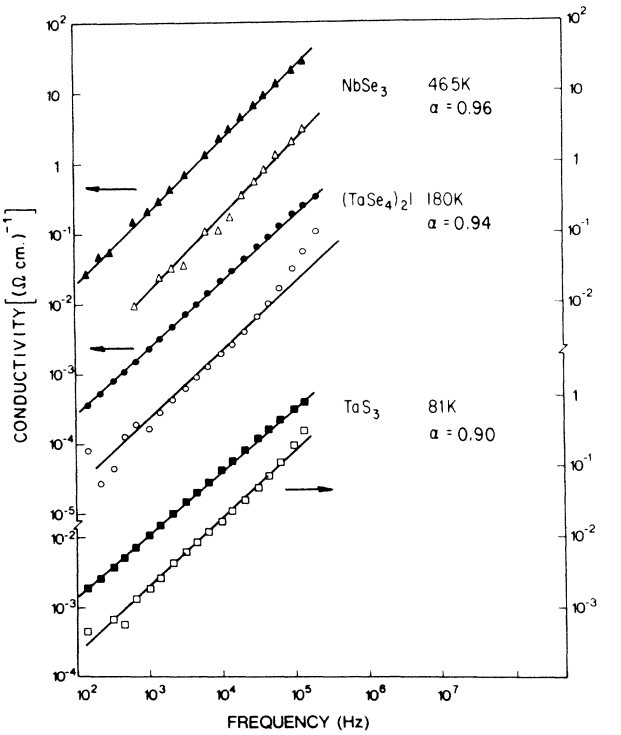

FIG. 4. Re$\sigma(\omega)$ and Im$\sigma(\omega)$ as the function of frequency for $NbSe_3$ at 46.5 K, $(TaSe_4)_2I$ at 180 K, and o-TaS_3 at 81 K. The solid lines are fits to Eq. (1) with exponents $\alpha=0.96$, 0.94, 0.90, respectively.

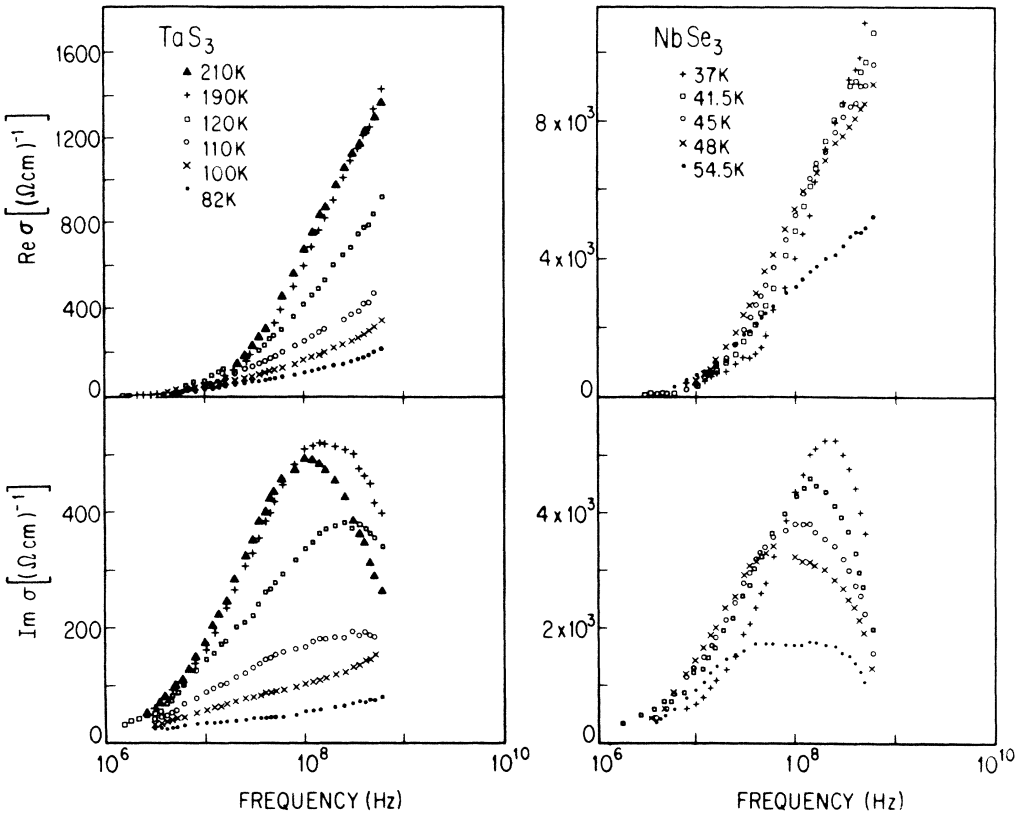

FIG. 5. The frequency-dependent conductivity observed in o-TaS_3 (left) and in $NbSe_3$ (right) at various temperatures.

III. RESULTS

The low-frequency conductivities, $\mathrm{Re}\sigma(\omega)$ and $\mathrm{Im}\sigma(\omega)$, measured by the low-frequency bridge configuration for $NbSe_3$ (below the second phase transition), for o-TaS_3, and for $(TaSe_4)_2I$ are displayed in Fig. 4. In all cases a power-law behavior is observed, and both $\mathrm{Re}\sigma(\omega)$ and $\mathrm{Im}\sigma(\omega)$ are proportional to ω^{α}, with $\alpha<1$, over an extended frequency range.

Fits to Eq. (1) are also displayed in the figure with $\alpha=0.96$ for $NbSe_3$ at 46.5 K, $\alpha=0.95\pm0.02$ for o-TaS_3 at 81 K, and $\alpha=0.94\pm0.02$ for $(TaSe_4)_2I$ at 180 K. The frequency-dependent conductivity of o-TaS_3 and $NbSe_3$, measured in a frequency range of 4—500 MHz, is presented in Fig. 5. For these two materials the crossover from low to high conductivity (with a peak in $\mathrm{Im}\sigma$), characteristic to overdamped response, is apparent. We did not find such crossover in $(TaSe_4)_2I$, and recent experiments indicate that for this compound the crossover frequency falls in the (10—100)-GHz range.[35]

The frequency dependence of the dielectric constant,

$$\epsilon(\omega)=4\pi\frac{\mathrm{Im}\sigma(\omega)}{\omega}\ , \tag{2}$$

is shown in Fig. 6. The saturation at low frequencies, suggested by the simple harmonic-oscillation description, was not observed. Instead, $\epsilon(\omega)$ continues to increase as $\omega\rightarrow0$, and in this limit $E(\omega)\sim\omega^{\alpha-1}$. It is also evident from Fig. 6 that the development of this low-frequency "cusp" is gradual as the frequency is decreased. We do not observe two separate relaxation processes which would separately characterize the low- and the high-frequency behavior of the frequency-dependent response; in this respect our results differ from those in $K_{0.3}MoO_3$.[15]

Further measurements of $\mathrm{Re}\sigma$ and $\mathrm{Im}\sigma$ were made in

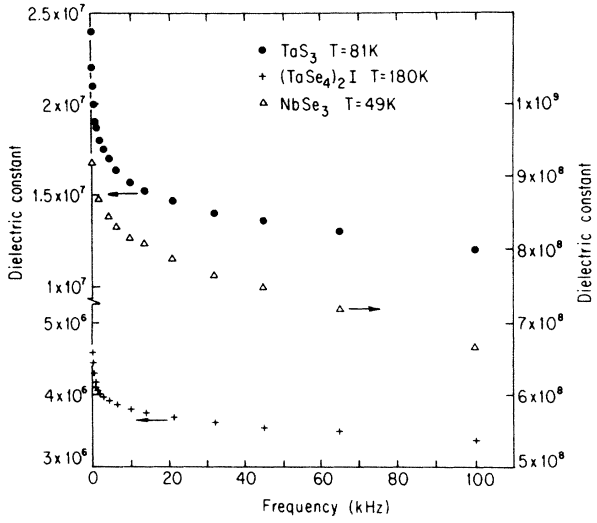

FIG. 6. The frequency dependence of the dielectric constant measured in $NbSe_3$, o-TaS_3, o-TaS_3, and $(TaSe_4)_2I$ at temperatures indicated on the figure.

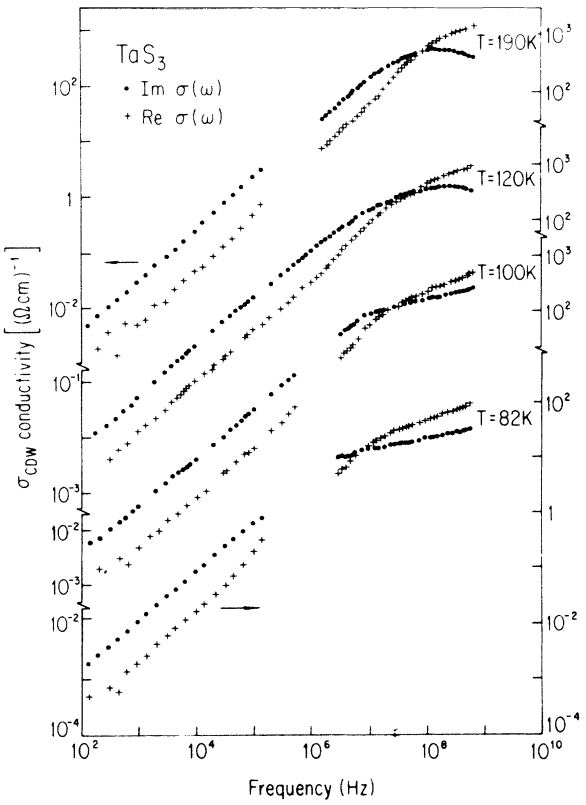

FIG. 7. Frequency-dependent conductivity observed in TaS_3 for several different temperatures.

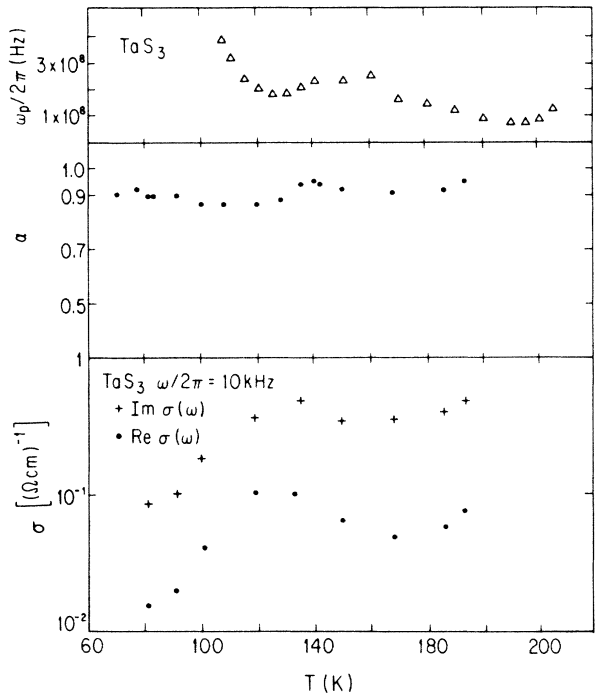

FIG. 8. Temperature dependence of the parameters α, $\mathrm{Im}\sigma(\omega=10\ \mathrm{kHz})$, and ω_p for o-TaS_3.

o-TaS_3 at many other temperatures; the results at four temperatures are shown in Fig. 7. Both $\mathrm{Im}\sigma(\omega)$ and $\mathrm{Re}\sigma(\omega)$ continue to decrease approximately at the same rate (see below) with decreasing frequency and do not show a flattening off in the $\omega\rightarrow 0$ limit. Power-law behavior was observed at all temperatures investigated, down to $T=42$ K. Power-law frequency dependence of conductivity was also reported by Zhilinskii *et al.*[12,17] at $T=4.3$ K with exponent $\alpha=0.83$. Similar overall behavior has been observed in o-TaS_3 by Kalem *et al.*[39] below 100 K, but at high temperatures they report a leveling off of $\epsilon(\omega)$ below about 1 MHz. It is obvious from Fig. 7 that we do not find such saturation, and ϵ continues to increase with decreasing ω down to 100 Hz at all temperatures. A possible reason for this disagreement is discussed in Sec. V.

While the dc conductivity of o-TaS_3 varies strongly with temperature, the frequency-dependent contribution has a relatively weak temperature dependence between 100 and 200 K. This feature of the data is more apparent when the parameters characterizing $\sigma(\omega)$ are plotted for several temperatures. Figure 8 shows the temperature dependence of the complex conductivity measured at 10 kHz, the exponent α, and the characteristic frequency ω_p at which $\mathrm{Im}\sigma(\omega)$ has the maximum. These parameters vary but no more than a factor of 4 between 100 and 190 K, while the dc conduction changes by a factor of approximately 100. In this range ω_p shows two dips, which correlate with two mild peaks in σ_{CDW} (10 KHz). These two peaks have previously been noticed in the 1-MHz dielectric constant in o-TaS_3 and have been proven to correspond to two dips in the temperature dependence of the threshold field for nonlinear conduction.[28] Also, a similar temperature dependence occurs in the microwave response.[3,27] Despite the frequent observation of this characteristic temperature dependence, its microscopic origin remains a mystery.

Figure 8 shows that below $\cong 100$ K both ω_p and σ_{CDW} change rapidly with temperatures. Also below 100 K, the microwave response shifts towards higher ω,[27,40] and the threshold field increases strongly.[41] It has been suggested that the threshold behavior below 100 K is due to lock-in of the CDW wave vector to a value commensurate with the underlying lattice.[42] It is expected that due to differences in pinning the dynamical response of a commensurate CDW is different from that of an incommensurate CDW. Local soliton excitations of the collective mode may play an important role in a situation where commensurability pinning is strong and shifts the oscillator response of the whole CDW mode to higher frequencies. Local excitations are also expected to lead to a strongly-temperature-dependent ac response.

In the discussion which follows, we focus on the frequency-dependent response of o-TaS_3 above approximately 100 K, where the response is due to an incommensurate charge-density wave, and commensurability effects are not expected to play an important role.

IV. ANALYSIS

In this section we consider the relevance of our results to several theoretical expressions. First we examine two common, phenomenological models for CDW conductivity, the "classical single-particle model" and the Zener tun-

neling theory. Next we consider improvements to the classical model by allowing distributions of parameters which characterize the frequency-dependent response. This is allied in spirit to popular approaches to glasses and localization, and the tunneling theory could be treated analogously. Finally, we take note of the recent "relaxational dynamics" CDW calculations using the Fukuyama-Lee-Rice Hamiltonian.

A. Comparison with the phenomenological models

The simplest classical treatment of charge-density-wave dynamics treats the collective mode as a rigid charged massive object whose dynamics is completely described by a single center-of-mass coordinate x. Then, in the absence of a dc field, the equation of motion for small amplitude ac fields is[22]

$$\ddot{x}+\frac{1}{\tau}\dot{x}+\omega_0^2 x+\frac{eEe^{i\omega t}}{m^*}\ , \tag{3}$$

where $1/\tau$ is a phenomenological damping constant and m^* is the effective mass of the condensate. Early studies indicated an overdamped response,[6,10] $\omega_0\tau \gg 1$, and consequently the frequency-dependent conductivity is given to a first approximation by

$$\mathrm{Re}\sigma(\omega)=\frac{ne^2\tau}{m^*}\frac{\omega^2}{\omega^2+(\omega_{co})^2}\ , \tag{4}$$

$$\mathrm{Im}\sigma(\omega)=\frac{ne^2\tau}{m^*}\frac{\omega_{co}}{\omega}\frac{\omega^2}{\omega^2+(\omega_{co})^2}\ . \tag{5}$$

Here n is the number of carriers in the collective mode and $\omega_{co}=\omega_0^2\tau$ is the crossover frequency. In Fig. 1 we showed both $\mathrm{Re}\sigma(\omega)$ and $\mathrm{Im}\sigma(\omega)$ measured in $NbSe_3$ below the second phase transition T_2. The solid lines in that figure correspond to Eqs. (4) and (5) with parameters given in the figure caption. (Similar fits were obtained for the ω-dependent response of o-TaS_3 and also in earlier studies of the frequency-dependent response.) While a good overall agreement between the experimental results and this single harmonic-oscillator description is evident, a closer inspection reveals deviations from Eqs. (4) and (5). In general, the observed ω dependence is less sharp, suggesting a distribution of pinning frequencies and/or relaxation times.

The deviations are more serious at low frequency where Eqs. (4) and (5) predict $\mathrm{Re}\sigma\approx\omega^2$ and $\mathrm{Im}\sigma\approx\omega$, but the data is better represented by ω^α, $\alpha\cong 0.9$, for both the in-phase and quadrature parts. Thus, at low frequency the experimental results exceed the predictions; for $\mathrm{Re}\sigma$ the discrepancy is by several orders of magnitude at the lowest frequency measured. This is illustrated in Fig. 9 for o-TaS_3 in a log-log representation which emphasizes the low-frequency response. The solid lines represent Eqs. (4) and (5) with parameters $\sigma_\infty=ne^2\tau/m^*=2100\ \Omega^{-1}\mathrm{cm}^{-1}$ and $\omega_{co}=\omega_0^2\tau=240\times 2\pi$ MHz.

Another approach is to interpret the strong dielectric

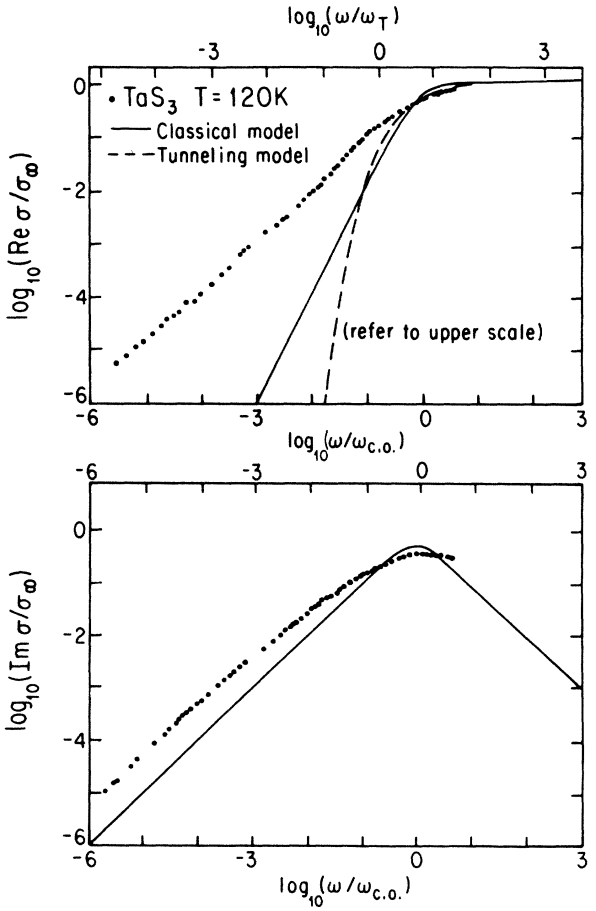

FIG. 9. Frequency-dependent $\mathrm{Re}\sigma(\omega)$ and $\mathrm{Im}\sigma(\omega)$ for o-TaS_3 at $T=120$ K, compared with the predictions of the phenomenological models. The solid lines are fits to the classical particle model with parameters $\sigma_\infty=2100\ (\Omega\,\mathrm{cm})^{-1}$ and $\omega_{co}=2\pi\times 240$ MHz. The dashed line is a fit to the tunneling model [Eq. (6)] with parameter $A=2100\ (\Omega\,\mathrm{cm})^{-1}$, $\omega_T=2\pi\times 26$ MHz.

response in terms of the tunneling model,[23] where the frequency dependence is due to collective excitations of the CDW condensate across a pinning gap $\Delta_p=\hbar\omega_p$. A model developed by Tucker[43] to treat the ac response of superconductor-insulator-superconductor tunnel junctions in the quantum limit is adopted to describe the frequency-dependent conductivity of CDW's.[44] This formalism leads to a scaling relation between the frequency and the dc electric-field-dependent response. If one assumes that only electric fields above E_T are effective,[11] the scaling relation is

$$\mathrm{Re}\sigma\left[\frac{\omega}{\omega_T}\right]=\sigma_{dc}\left[\frac{E-E_T}{E_T}\right]\ , \tag{6}$$

where the electric-field-dependent part of the dc conduction is described by

$$\sigma_{dc}=A\left[1-\frac{E_T}{E}\right]\exp\left[-\frac{E_0}{E}\right]\ . \tag{6'}$$

Here E_T is the threshold field at which nonlinear conduction occurs, A and E_0 are parameters, determined experimentally. This expression takes into account the observation that there is no threshold frequency for the onset of ω-dependent response. Equation (6) works well at high frequencies, but once again at low frequencies serious deviations from the predicted ω dependence develop. A fit to Eq. (6) demonstrating this point is shown as the dotted line in Fig. 9. The fit was produced by applying the scaling rule, Eq. (6), to the form of the dc current-voltage relationship given as Eq. (12) of Ref. 44.

Thus the description of $\sigma(\omega)$ over a broad range of frequencies, both in terms of the classical single-particle model and in terms of the tunneling description of CDW dynamics, leads to an appropriate fit in various materials only at frequencies exceeding approximately 10 MHz.[6,10,11] However, these models fail to account for both $\mathrm{Re}\sigma(\omega)$ and $\mathrm{Im}\sigma(\omega)$ at low frequencies, where the measured conductivities exceed the calculated values. There appears to be an excess contribution to the ac response in the $\omega\rightarrow 0$ limit.

The most likely explanation for the breakdown of the above descriptions in the low-frequency limit is that the details of the pinning, caused by random impurities, are not explicitly considered. Consequently, the ω-dependent response is characterized by a single energy scale in both models, by ω_T in terms of the tunneling model and by $\omega_0^2\tau$ for the description in terms of a purely classical response. Apparently the experimental results call for a more complete treatment of CDW pinning. Because of the aspect of randomness, proper treatment of the pinning and the resulting frequency-dependent conductivity is quite difficult. In the rest of this section we present various approximations to an improved interpretation of the conductivity.

B. Distributions of parameters

The response represented by Eq. (1) is commonly observed in disordered systems, and in particular in glasses, where $\alpha\approx 0.8$.[29] The observed $\sigma(\omega)$ may be regarded as a broad superposition of Debye responses, Eqs. (4) and (5); however, the distribution functions which determine the weights of the various Debye curves have usually been treated phenomenologically or on the basis of convenience. One complicated distribution function gives the popular Cole-Cole expression[30] for the dielectric constant:

$$\epsilon(\omega)=\frac{\epsilon_0}{1+(i\omega\tau_0)^{1-\alpha}} . \tag{7}$$

A more complicated, three-parameter distribution function[45] leads to

$$\epsilon(\omega)=\frac{\epsilon_0}{[1+(i\omega\tau_0)^{1-\alpha}]^{\beta}} . \tag{8}$$

As the underlying distributions contain no physical significance, we will not describe them here. The form of Eq. (8) (with free parameters ϵ_0, τ_0, α, and β) has been applied to describe the frequency-dependent dielectric constant in $K_{0.3}MoO_3$ (Ref. 15) and o-TaS_3 (Ref. 39) with some success. In the same spirit, we previously used the form[16]

$$\sigma(\omega)=\sigma_\infty\frac{(i\omega\tau_0)^{\alpha}}{1+(i\omega\tau_0)^{\alpha}} \tag{9}$$

to account for our experimental findings in o-TaS_3. Although we make no attempt to justify this expression microscopically, it is also suggestive of a distribution of relaxation times. In contrast to Eqs. (7) and (8), Eq. (9) leads to a power law, Eq. (1), for $\omega\rightarrow 0$, and also leads to $\mathrm{Re}\sigma(\omega\rightarrow\infty)=\sigma_\infty$ in the large frequency limit. At high frequencies, however, Eq. (9) deviates dramatically from the measured frequency-dependent response. Figure 10 shows $\sigma(\omega)$ for TaS_3 at 120 K represented in the complex conductivity plane. The solid line (which is a segment of a tilted circle) is the best fit to Eq. (9). The value of $\alpha(=0.87)$ can be deduced from the tilt angle, as shown in the figure. At low frequencies Eq. (9) reduces to Eq. (1). Thus the fit is quite reasonable, but (as already remarked) it seems to be devoid of physical content.

Interestingly, there exists a very simple distribution of Debye responses which represents the data quite well without requiring α as a parameter. Suppose that $\omega_{co}=\omega_x$, the characteristic frequency of the Debye

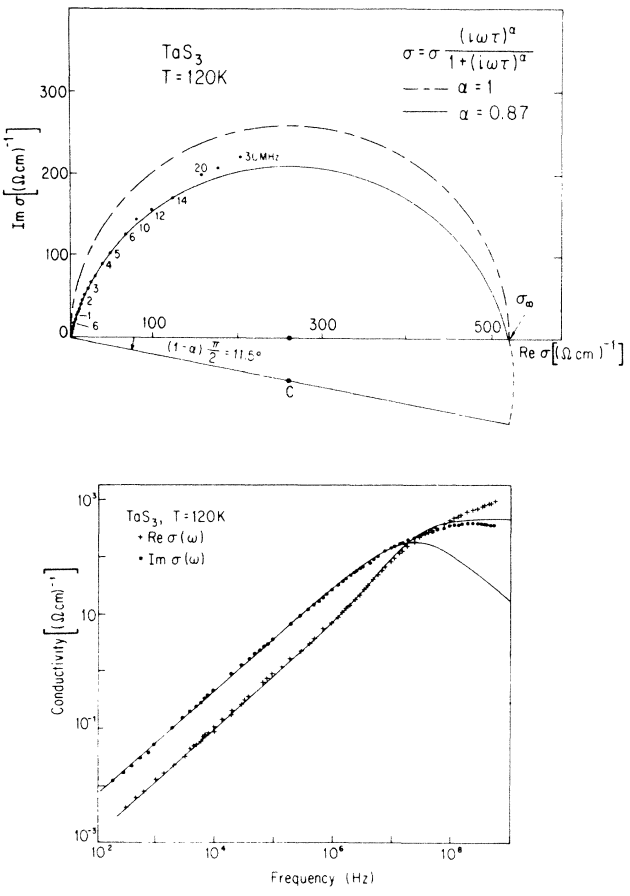

FIG. 10. (a) $\mathrm{Re}\sigma(\omega)$ and $\mathrm{Im}\sigma(\omega)$ for TaS_3 at 120 K plotted on the complex conductivity plane, a Cole-Cole–like plot. The solid tilted semicircle is a fit to Eq. (9) with parameters α,σ_∞ determined by the tilt angle and by the intersection with the $\mathrm{Re}\sigma(\omega)$ axis, respectively, as shown in the figure. (b) A equivalent representation of the above data and the fits to Eq. (9). $\omega_{co}=2\pi\times 25$ MHz, α and σ_∞ are the same as before.

response is distributed uniformly from zero to an upper cutoff ω_{max}. Then

$$\sigma(\omega)=\sigma_\infty \int \frac{i\omega}{\omega_x+i\omega}p(\omega_x)d\omega_x$$
$$=\frac{\sigma_\infty}{\omega_{max}}\int_0^{\omega_{max}}\frac{i\omega}{\omega_x+i_\omega}d\omega_x$$
$$=\sigma_\infty\frac{\omega}{\omega_{max}}\left[\tan^{-1}\left[\frac{\omega}{\omega_{max}}\right]+i\tfrac{1}{2}\ln\left[1+\frac{\omega^2}{\omega_{max}^2}\right]\right]. \quad (10)$$

Figure 11 shows the fit to the data. For $\omega \ll \omega_{max}$, Eq. (10) becomes

$$\sigma(\omega)=\frac{\pi}{2}\sigma_\infty\left[\frac{\omega}{\omega_{max}}\right]+i\sigma_\infty\left[\frac{\omega}{\omega_{max}}\right]\ln\left[\frac{\omega}{\omega_{max}}\right]. \quad (11)$$

We do not claim any unique significance for these results, but they provide a clue to the underlying physics. Both the notion that something is distributed all the way to zero and the specific form of the imaginary part (a power law with logarithmic correction) reminds us of hopping conductivity in localized systems.[32]

C. "Hopping" conductivity

The main features of impurity pinning can be described by the phase Hamiltonian,[46] which in one dimension is

$$H=\frac{\hbar v_F}{4\pi}\int\left[\left[\frac{d\phi}{dx}\right]^2+\left[\frac{1}{u_s}\frac{d\phi}{dt}\right]^2\right]dx$$
$$+V_0\rho_0\sum_i\cos[2k_Fx_i+\phi(x_i)], \quad (12)$$

where v_F and k_F are the Fermi velocity and wave vector, ρ_0 and ϕ are the amplitude and phase of the CDW, and the summation is over random impurity sites i. V_0 is the short-range impurity potential and u_s is the phason velocity, which is related to the effective mass m^* of the condensate by $u_s=(m/m^*)^{1/2}v_F$. The dimensionless parameter

$$\eta=\frac{V_0\rho_0}{v_Fn_i\hbar}, \quad (13)$$

where n_i is the number of impurities per unit length, separates regions where the effect of pinning is qualitatively different. When $\eta \gg 1$ (i.e., the pinning is strong relative to the deformability of the CDW phase) the phase is completely adjusted at every impurity site to obtain a maximum potential-energy gain. The phase-phase correlation length is of order $\bar{l}=1/n_i$, the average spacing between impurities. For $\eta \ll 1$ the phase is adjusted over a length scale L_0 large compared to $\bar{l}$. Scaling arguments, which neglect short-range perturbation around the impurities, lead to

$$L_0=(\pi^2\hbar^2v_F^2/n_i\rho_0^2V_0^2)^{1/3}$$

in one dimension.

For strong impurity pinning, the frequency-dependent response can easily be calculated in one dimension in the low-frequency limit. In this case the ac response is that of the sum of the individual, interrupted chain segments. Each segment may be regarded as a charged oscillator. As shown by Fukuyama and Lee,[46] the distribution of impurity spacings implies the following probability distribution of oscillator frequencies:

$$P(\omega_0)=\frac{\omega_{av}}{\omega_0^2}\exp\left[-\frac{\omega_{av}}{\omega_0}\right], \quad (14)$$

where

$$\omega_{av}=2\pi u n_i \quad (15)$$

is the average oscillator frequency. If the individual oscillators are assumed to be underdamped, the low-frequency conductivity becomes[46]

$$\mathrm{Re}\sigma(\omega)=\frac{2\pi^2u^2L_0}{v_F}\frac{\omega_{av}}{\omega^2}\exp\left[-\frac{\pi\omega_{av}}{\omega}\right]. \quad (16)$$

Where u is the phason velocity, v_F is the Fermi velocity, and $L_0\approx 1/n_i$ is the Fukuyama-Lee length. The arguments may be generalized including a phenomenological damping which describes the overdamped nature of the oscillators. The integral over the probability distribution [Eq. (14)] and the overdamped oscillator response [Eq. (4)] cannot be expressed in a simple analytical form; however, the low-frequency limit can be evaluated, and $\mathrm{Re}\sigma \sim \omega^2$ is obtained for $\omega \ll \omega_{av}$.

In the weak pinning case $\epsilon \ll 1$, examination of the energy dependence of the density of states of Eq. (12) gives the result[34]

$$\mathrm{Re}\sigma(\omega)=\frac{e^2u^2}{v_F\omega^*}\left[\frac{\omega}{\omega^*}\right]^2\ln^2\left[\frac{\omega^*}{\omega}\right], \quad (17)$$

which corresponds to the Mott-Berezhinskii result for one-dimensional localization.[32] The characteristic frequency ω^* is related to the pinning energy V_0 and is given in one dimension by

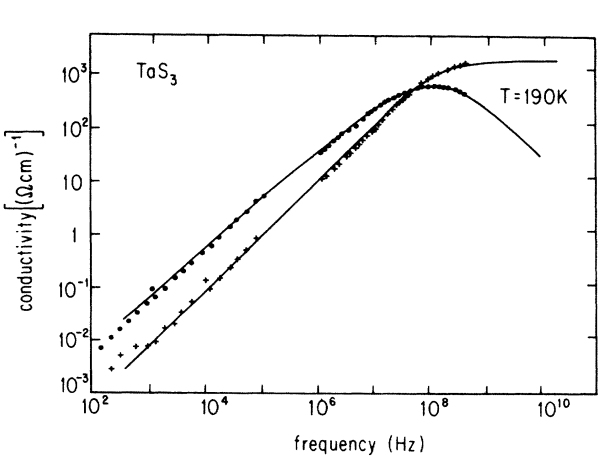

FIG. 11. The low-frequency $\mathrm{Re}\sigma(\omega)$ and $\mathrm{Im}\sigma(\omega)$ for TaS_3 at $T=190$ K, compared with Eq. (10).

$$\omega^* = (2\pi u/v_F)(n_i v_F V_0^2/2\pi)^{1/3} = \frac{u}{L_0}\left[\frac{2\pi^2\hbar}{\rho_0}\right]^{2/3}, \quad (18)$$

where L_0 is the Fukuyama-Lee length defined above. Equation (17) is appropriate if $\omega_1 < \omega < \omega^*$ with $\omega_1 = V_0 u/v_F$. Below this frequency the conductivity reverts to the form of Eq. (16). We have argued in Ref. 16 that the range of validity of Eq. (17) is very limited.

In Fig. 12 the experimental behavior is compared to the predictions based on Eq. (16) and (17). The Mott-Berezhinskii law predicts that $\omega^{-1}[\mathrm{Re}\sigma(\omega)]^{1/2}$ versus $\ln\omega$ is linear, while if Eq. (16) is appropriate, $\ln[\mathrm{Re}\sigma(\omega)]$ is a linear function of ω^{-1}. It is obvious from the figure that neither of these behaviors is observed.

The expressions Eqs. (17) and (18) are relevant for a collection of oscillator states ϵ_i with potential-energy barriers U_{ij} between them.[32] The dielectric absorption at ω [and the consequent contribution to $\sigma(\omega)$] comes from direct, electric-dipole transitions between ϵ_i and ϵ_j, $\epsilon_j - \epsilon_i = \hbar\omega$. The absorption will have an additional contribution from relaxational processes in which phonons (or phasons) try to maintain equilibrium between oscillator states while the applied low-frequency electric field modulates the energy levels. For the case of electron localization in three dimensions, the expression for $\sigma(\omega)$ is reduced by one power of ω and becomes temperature dependent (because of the role of thermal phonons).[32] Carrying over the localization results to the present, one-dimensional situation, we expect

$$\mathrm{Re}\sigma(\omega) \sim kT\left[\frac{\omega}{\omega^*}\right]\ln^2\left[\frac{\omega^*}{\omega}\right]. \quad (19)$$

Furthermore, because direct photon transitions are no longer involved, we do not expect this formula to have the limited range of validity of Eq. (17).

Motivated by our experimental findings Gor'kov has recently proposed[47] that the results obtained for localization in random systems in the presence of Coulomb interactions[48] may be applicable to CDW materials. The presence of Coulomb forces modifies the low-frequency limit of the Mott-Berezhinskii law to become

$$\mathrm{Re}\sigma(\omega) \sim \omega \ln^2\omega . \quad (19')$$

As shown in Fig. 13, this form fits the data. However, like Eq. (17), it is expected to break down in the $\omega \to 0$ limit. Also, if Coulomb effects are important, a different behavior might be expected for o-TaS_3 and $(TaSe_4)_2I$, which become semiconductors below their Peierls transitions, and for $NbSe_3$, where only a fraction of the electrons are condensed into the CDW mode. Figures 4 and 5 demonstrate that no such difference was observed.

D. Relaxational dynamics approach

Finally, we consider approaches in which the Hamiltonian, Eq. (12), is used in a completely classical and dissipative equation of motion:[31,35]

$$\frac{1}{\Gamma}\frac{d\phi(\mathbf{r})}{dt} = \left[\frac{\delta H}{\delta\phi(\mathbf{r})} + \frac{neE}{2k_F}\right], \quad (20)$$

where Γ is the damping constant and E is the applied electric field. This approach leads to metastable states: For a fixed electric field, there exist several states which are close in energy, but separated in configuration space by potential barriers.[31] The corresponding static phase configurations, $\phi_i(x)$, tend to differ from one another by containing of 2π phase slips. The distribution of barrier

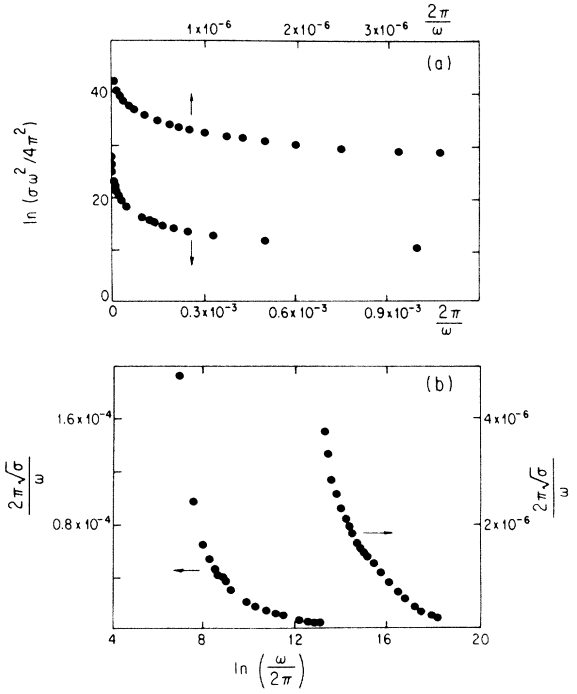

FIG. 12. Low-frequency $\mathrm{Re}\sigma(\omega)$ for TaS_3 at $T = 120$ K, compared with Eqs. (16) and (17). Equation (17) predicts that $\omega^{-1}[\mathrm{Re}\sigma(\omega)]^{1/2}$ versus $\ln\omega$ is linear, while if Eq. (16) is appropriate, $\ln[\omega^2\mathrm{Re}\sigma(\omega)]$ is a linear function of ω^{-1}. Neither of these behaviors is observed.

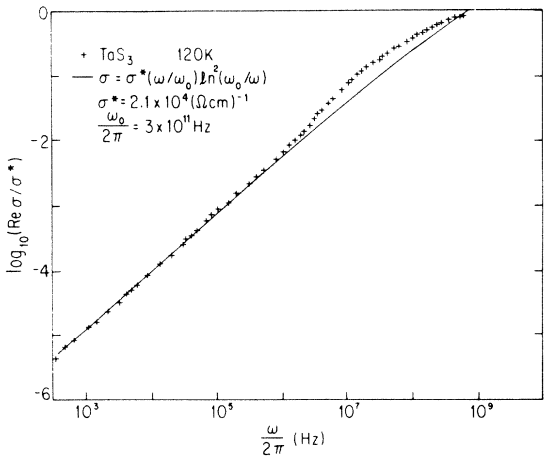

FIG. 13. Low-frequency $\mathrm{Re}\sigma(\omega)$ for o-TaS_3 at 120 K, compared with the prediction of the modified Mott-Berezhinskii law, considering strong Coulomb interactions, Eq. (19').

heights between the various ϕ_i extends to zero, and therefore large local responses to the applied low-frequency electric field are likely. The models predict a cusp in the dielectric constant, and

$$\epsilon(\omega)=\epsilon(\omega=0)-|\omega|^{\alpha'} . \quad (21)$$

In a one-dimensional mode-coupling calculation, $\alpha'=\frac{1}{2}$,[31] while a three-dimensional treatment of the depinning as a dynamical critical phenomenon gives $\alpha'=1$.[35] The experimental data (Fig. 6) may be consistent with a finite cusp with $\alpha'<1$; however, even below 100 Hz the measured $\epsilon(\omega)$ is continuing to diverge with decreasing ω.

Metastable states and relaxation effects due to transitions are also considered in the single-domain dynamics approach.[49] While the high-frequency response obtained is similar to models which take the internal deformations into account, the low-frequency behavior has not been considered. The existence of metastable states, within the framework of the model, suggests a cusplike behavior of $\epsilon(\omega\rightarrow 0)$. The zero-frequency cusp, predicted by these calculations, was observed by Cava *et al.* in $K_{0.3}MoO_3$.[15]

The models therefore explain, at least qualitatively, our experimental findings, and make a clear connection between the enhanced low-frequency ac response and the existence of metastable states. In contrast to the nonuniversal behaviors observed experimentally, they, however, predict well-defined exponents which also depend on the dimensionality of the system.

V. CONCLUSIONS

The principal experimental result uncovered in this investigation is the power-law frequency dependence of the small-amplitude, low-frequency complex conductivity. This behavior has been observed in $NbSe_3$, orthorhombic TaS_3, and $(TaSe_4)_2I$ and over a broad range of frequency and at several widely differing temperatures. The power-law behavior disagrees conspicuously with both the classical single-particle model and with the tunneling theory.

These results are similar to the dielectric behavior of glasses and other random systems, and they demonstrate that disorder plays an essential role in the low-frequency dynamics of the pinned CDW mode. Disorder effects are a natural consequence of pinning by random impurities. Random impurity distribution, combined with the fundamental periodicity of the collective mode (which allows phase adjustments and 2π phase slips), leads to metastable states and to a broad distribution of local pinning energies.

In order to calculate $\sigma(\omega)$ beginning with the notion of metastable states, the distribution of the states must be known or guessed. Two general types of calculations have been made. One type considers tunneling through potential barriers $U>kT$ separating spatially distant levels. The approach and results are similar to the localization problem and give reasonable approximations to power-law conductivity, $\sigma\sim\omega^{\alpha}$, $\alpha\simeq 0.9$, in agreement with the data. The other type considers excitation over short barriers, $U\leq kT$, separating spatially adjacent configurations. The resulting dielectric constant has a cusp at $\omega=0$, in qualitative agreement with measurements. In both cases, we can form a picture of localized $\pm 2\pi$ phase slips (as described by Littlewood[31] and Matsukawa and Takayama[50]) shifting back and forth in response to the applied, low-frequency electric field.

The qualitative agreement of our experimental results with these model calculations indicates that electric-field-induced shifts of the phase slips are essential in the overall frequency-dependent response. Consequently, the ac conductivity is also expected to be strongly dependent on the amplitude of an ac driving field: $\mathrm{Re}\sigma(\omega)$ and $\mathrm{Im}\sigma(\omega)$ should increase for increasing U_{ac}. Investigation of the response to pulsed electric fields indeed shows orders of magnitude higher dielectric constant for fields close to E_T.[36,51] The experimental results presented here are obtained in the small ac signal limit, and these results were found to be independent of U_{ac} within experimental error. Yet due to the broad distribution of local barrier heights, extending down to zero, a true small signal limit does not in principle exist.

We are aware of the disagreement between our experimental findings and those made by others on the same or on related systems. Specifically, Cava *et al.*[15] and Ong *et al.*[20] see a saturation in $\epsilon(\omega)$ and a flattening off in $\mathrm{Re}\sigma(\omega)$ at low frequencies, but in the same frequency regime where we still observe a diverging dielectric response as shown in Fig. 6. The reason for this disagreement is not clear at present. One source of disagreement lies in the intrinsic nonlinearity of the response, and the observed frequency-dependent conductivity depends on the amplitude of the ac signal down (in principle) to very low amplitudes. The other possible source is the difference in the measurement configuration employed: while in our studies the dc response was first subtracted, and the resulting signal was analyzed, in studies conducted by others the full response was analyzed, and the dc part was subtracted subsequently. If the signal processing electronics performs an accurate Fourier analysis on the measured (nonlinear) response, then the two methods give identical results. However, widely different results may be obtained by lock-in amplifiers, impedance bridges, and network analyzers; depending on the particular method, these devices handle the nonlinear signal. The detailed investigation of the nonlinear response may lead to a deeper understanding of the microscopic processes behind the giant dielectric response of these materials.

Our results also have an intimate relation to the long-time relaxation phenomena which occur following a thermal quench or electric field pulse.[37,52] Such relaxation effects in o-TaS_3 are described by a time-dependent polarization of the approximate form

$$P(t)\sim\ln(t/\tau) . \quad (22)$$

Logarithmic time decays are also often observed in spin glasses and other random systems and follow logically from a distribution of barriers extending to zero. We anticipate that the investigation of the dielectric relaxation in the time domain, complementary to the frequency-dependent response reported here, will be a fruitful area for further studies.

ACKNOWLEDGMENTS

The samples used in this study were prepared by M. Maki and B. Alavi. Discussions with P. Littlewood, D. S. Fisher, R. M. Fleming, and J. R. Tucker are gratefully acknowledged. This work was supported by National Science Foundation Grant No. DMR-81-21394.

---

†Permanent address: Central Research Institute for Physics, P. O. Box. 49, H-1525 Budapest, Hungary.

*Present address: Department of Physics, University of Illinois at Urbana-Campaign, Urbana, IL 61801.

[1]See, for example, G. Gruner and A. Zettl: Phys. Rep. **119**, 117 (1985).

[2]For recent developments, see *Charge Density Waves in Solids,* Vol. 217 of *Lecture Notes in Physics,* edited by Gy. Hutiray and J. Solyom (Springer-Verlag, Berlin, 1985).

[3]G. Gruner, L. C. Tippie, J. Sanny, W. G. Clark, and N. P. Ong, Phys. Rev. Lett. **45**, 935 (1980).

[4]S. W. Longcor and A. M. Portis: Bull. Am. Phys. Soc. **25**, 340 (1980).

[5]J. C. Gill, Solid State Commun. **37**, 459 (1981).

[6]G. Gruner, A. Zettl, W. G. Clark, and John Bardeen, Phys. Rev. B **24**, 7247 (1981).

[7]C. M. Jackson, A. Zettl, G. Gruner, and A. H. Thompson, Solid State Commun. **39**, 531 (1981).

[8]A. Zettl and G. Gruner, Phys. Rev. B **25**, 2081 (1982).

[9]G. Gruner, Mol. Cryst. Liq. Cryst. **81**, 17 (1982).

[10]A. Zettl, C. M. Jackson, and G. Gruner, Phys. Rev. B **26**, 5773 (1982).

[11]J. H. Miller, J. Richard, J. R. Tucker, and John Bardeen, Phys. Rev. Lett. **51**, 1592 (1983).

[12]S. K. Zhilinskii, M. E. Itkis, F. Ya. Nad', I. Ya. Kalnova, and V. B. Preobrazhenskii, Zh. Eksp. Teor. Fiz. **85**, 362 (1983) [Sov. Phys.—JETP **58**, 211 (1983)].

[13]M. Maki, M. B. Kaiser, A. Zettl, and G. Gruner, Solid State Commun. **46**, 497 (1983).

[14]R. E. Thorne, W. G. Lyons, J. H. Miller, J. Richard, and J. R. Tucker, Solid State Commun. **50**, 833 (1984).

[15]R. J. Cava, R. M. Fleming, P. Littlewood, E. A. Rietman, L. F. Schneemeyer, and R. G. Dunn, Phys. Rev. B **30**, 3228 (1984).

[16]Wei-Yu Wu, L. Mihaly, G. Mozurkewich, and G. Gruner, Phys. Rev. Lett. **52**, 2382 (1984).

[17]S. K. Zhilinskii, M. E. Itkis, and F. Ya. Nad, Phys. Status Solidi **81**, 367 (1984).

[18]G. Gruner, Proceedings of the International Conference on Low Dimensional Conductors, Sapporo, 1983 (unpublished).

[19]R. P. Hall, M. Sherwin, and A. Zettl, in Ref. 2, p. 314.

[20]N. P. Ong, G. Verma, and X. J. Zhang, in Ref. 2, p. 296.

[21]Wei-Yu Wu, L. Mihaly, G. Mozurkewich, and G. Gruner, in Ref. 2, p. 311.

[22]G. Gruner, A. Zawadowski, and P. M. Chaikin, Phys. Rev. Lett. **46**, 511 (1981).

[23]John Bardeen, Phys. Rev. Lett. **42**, 1498 (1980); **45**, 1978 (1981).

[24]A. Zettl, G. Gruner, and A. H. Thompson, Phys. Rev. B **26**, 5760 (1982).

[25]J. H. Miller, J. Richard, R. E. Thorne, W. G. Lyons, and J. Bardeen, Phys. Rev. B **29**, 2328 (1984).

[26]D. Reagor, S. Sridhar, and G. Gruner, in Ref. 2, p. 308, S. Sridhar, D. Reagor, and G. Gruner, Phys. Rev. Lett. **55**, 1196 (1985).

[27]G. Mihaly, L. Mihaly, and H. Mutka, Solid State Commun. **49**, 1009 (1984).

[28]Wei-Yu Wu, A. Janossy, and G. Gruner, Solid State Commun. **49**, 1013 (1984).

[29]A. K. Jonsher, J. Mater. Sci. **16**, 2037 (1981); K. L. Ngai and Fu-Sui Lin, Phys. Rev. B **24**, 1049 (1981).

[30]K. S. Cole and R. H. Cole, J. Chem. Phys. **9**, 341 (1941).

[31]P. Littlewood, in Ref. 2, p. 369.

[32]N. F. Mott, Adv. Phys. **16**, 49 (1961); V. L. Berezhinskii, Zh. Eksp. Teor. Fiz. **65**, 1251 (1973) [Sov. Phys.—JETP **38**, 620 (1974)].

[33]N. F. Mott and Davis, *Electronic Processes in Noncrystalline Materials* (Clarendon, Oxford, 1979).

[34]M. V. Feigelman and V. M. Vinokur: Phys. Lett. **87A**, 53 (1981); Solid State Commun. **45**, 603 (1983).

[35]D. S. Fisher, Phys. Rev. B **31**, 1396 (1984).

[36]G. Mihaly, Gy. Hutiray, and L. Mihaly, Solid State Commun. **48**, 203 (1983).

[37]G. Mihaly and L. Mihaly, Phys. Rev. Lett. **52**, 149 (1984).

[38]R. M. Fleming, L. F. Schneemeyer, and R. J. Cava, Phys. Rev. B **31**, 1181 (1985); R. J. Cava, R. M. Fleming, R. G. Dunn, and E. A. Rietman, *ibid.* **31**, 8325 (1985).

[39]C. B. Kalem, N. P. Ong, and J. C. Eckert (unpublished).

[40]W. W. Fuller, G. Gruner, P. M. Chaikin, and N. P. Ong, Phys. Rev. B **23**, 6259 (1981).

[41]A. W. Higgs and J. C. Gill, Solid State Commun. **47**, 737 (1983); G. Mihaly, Gy. Hutiray, and L. Mihaly, Phys. Rev. B **28**, 4896 (1983).

[42]C. Roucau, R. Ayroles, P. Monceau, L. Guemas, A. Meerschaut, and J. Rouxel, Phys. Status Solidi **62**, 483 (1980).

[43]J. Tucker, IEEE J. Quant. Electron **QE-15**, 1234 (1979).

[44]J. H. Miller, J. Richard, J. R. Tucker, and John Bardeen, Phys. Rev. Lett. **51**, 1592 (1983).

[45]S. Havrikiak and S. Negami, Polymer **8**, 161 (1967).

[46]K. B. Efetov and A. I. Larkin, Zh. Eksp. Teor. Fiz. **72**, 2350 (1977) [Sov. Phys.—JETP **45**, 1236 (1977)]; H. Fukuyama and P. A. Lee, Phys. Rev. B **17**, 535 (1978); P. A. Lee and T. M. Rice, *ibid.* **19**, 3970 (1979).

[47]L. P. Gor'kov (private communication).

[48]B. L. Shklovski and A. L. Éfros, Zh. Eksp. Teor. Fiz. **84**, 406 (1981) [Sov. Phys.—JETP **54**, 218 (1981)].

[49]R. A. Klemm and J. R. Schrieffer: Phys. Rev. Lett. **51**, 47 (1984).

[50]H. Matsukawa and H. Takayama, Solid State Commun. **50**, 283 (1984).

[51]G. Mihaly and L. Mihaly, Solid State Commun. **48**, 449 (1983).

[52]R. M. Fleming and L. F. Schneemeyer, Phys. Rev. B **28**, 6996 (1983).